SSRG International Journal of Electrical and Electronics Engineering
ISSN: 2348-8379/ https://doi.org/10.14445/23488379/IJEEE-V11I5P111

Volume 11 Issue 5, 119-128, May 2024

Original Article

ANFIS Based Control Strategy for Three-Level Converter-Based Solar PV Integrated UPQC of Distribution Power System Power Quality Problems

G. Sravanthi[1,4], T. Rama Subba Reddy[2], K. Mercy Rosalina[3]

[1,3]*Department of Electrical & Electronics Engineering, VFSTR University, Andhra Pradesh, India.*
[2,4]*Department of Electrical & Electronics Engineering, Vignan Institute of Technology & Science, Telangana, India.*

[1]*Corresponding Author : gsravanthi244@gmail.com*

Received: 07 March 2024 Revised: 08 April 2024 Accepted: 06 May 2024 Published: 29 May 2024

Abstract *- The majority of electric power quality problems have been effectively mitigated by the use of unified power quality conditioners, or UPQCs. Transformation techniques are used in conventional control schemes like P-Q theory-based control and Synchronous Reference Fame (SRF). Thus, they necessitate expensive DSPs and FPGAs and involve intricate computations. Reducing the size and operational difficulty of the control system is facilitated by the use of artificial intelligence control systems. For efficient operation and control, an ANN and ANFIS controller for UPQC is proposed in this article. The ANN controller decreases the system's cost and complexity. The analysis is done on the controller performance under different scenarios, such as load imbalances, voltage sag and swell, and harmonics in the supply voltage and load current. The ANFIS controller outperforms traditional controllers, according to the results.*

Keywords *- UPQC, Power Quality, ANFIS, Power Distribution System, Series APF, Shunt APF, MATLAB/Simulink.*

1. Introduction

The power system in the modern world is heavily integrated with electronic and non-linear equipment. Harmonics and numerous other power quality problems are increasing with the number of these devices and loads, necessitating the development of innovative mitigating devices with quicker control systems. Although passive filters may resolve harmonics, their size and cost make them cumbersome. Furthermore, poor design raises the harmonics and causes resonance [1].

In addition to eliminating resonance, active power filters resolved harmonic-related problems without being cumbersome or costly. Most PQ problems were resolved by the more sophisticated Unified Power Quality Conditioner (UPQC), which had a shunt and series APF connected back-to-back via a DC link capacitor [2, 3]. UPQC can achieve significantly higher performance by utilizing multi-level inverters as APFs.

This is because MLIs' lower switching frequency device operating compatibility and lower power electronic switch rating allow them to produce more sinusoidal output at rising levels, resulting in lower error, low dv/dt, and reduced losses during switching. Diode-clamped converter-type MLIs are commonly utilized in utility power systems because they may be associated back-to-back. However, in UPQC applications, the DC link capacitor voltage imbalance in this design results in suboptimal lower performance [4].

Either an additional hardware circuit for voltage balancing [5] or appropriate switching control [6, 7] must be utilized to prevent this imbalance. This raises the system's cost and complexity. Controllers such as PI, PID, fuzzy logic, etc., were employed to maintain a constant DC link voltage, but they all required precise linear mathematical models. Underload parameter modifications lead to unsatisfactory outcomes when the hard-to-design models are not developed [8].

PQ theory was applied to generate estimated reference signals for compensation, and its performance with a sinusoidal source was found to be satisfactory. Any system's performance will suffer if the source contains harmonics. Better performance could be obtained with or without source harmonics using an SRF-based control approach.

When the source had harmonics, later pq-theory combined with the harmonic extraction approach might also provide better performance than SRF did. These methods are also simple to use. However, these two approaches required extensive and intricate mathematical computations. The

performance was unsatisfactory when there were extreme harmonic circumstances. Artificial Intelligence (AI) is the control strategy of the new generation that aims to imbue robots and devices with human-like intelligence. Artificial Neural Networks (ANN) are one of the AI techniques that have gained the most traction in power electronics systems because of their ability to respond quickly to changes in the system's dynamics without compromising stability throughout a broad range of operations [9-12]. In order to enhance the reliability of the power distribution network with non-linear load amid corrupted source voltage, sag/swell, a 3-level converter fed UPQC is proposed in this work. Multi-layered feed-forward Artificial Neural Network (ANN) is used for controlling the current in the shunt APF by the three-level converters dependent UPQC, which also produces approximated signal references of current and voltage. Utilizing the Levenberg-Marquardt algorithm, the ANN model is trained. The purpose of the MATLAB/Simulink simulations is to assess the Controller's performance. Voltage sag and swell, harmonic abatement, DC-link voltage balancing, and %THD will all be analysed in this paper.

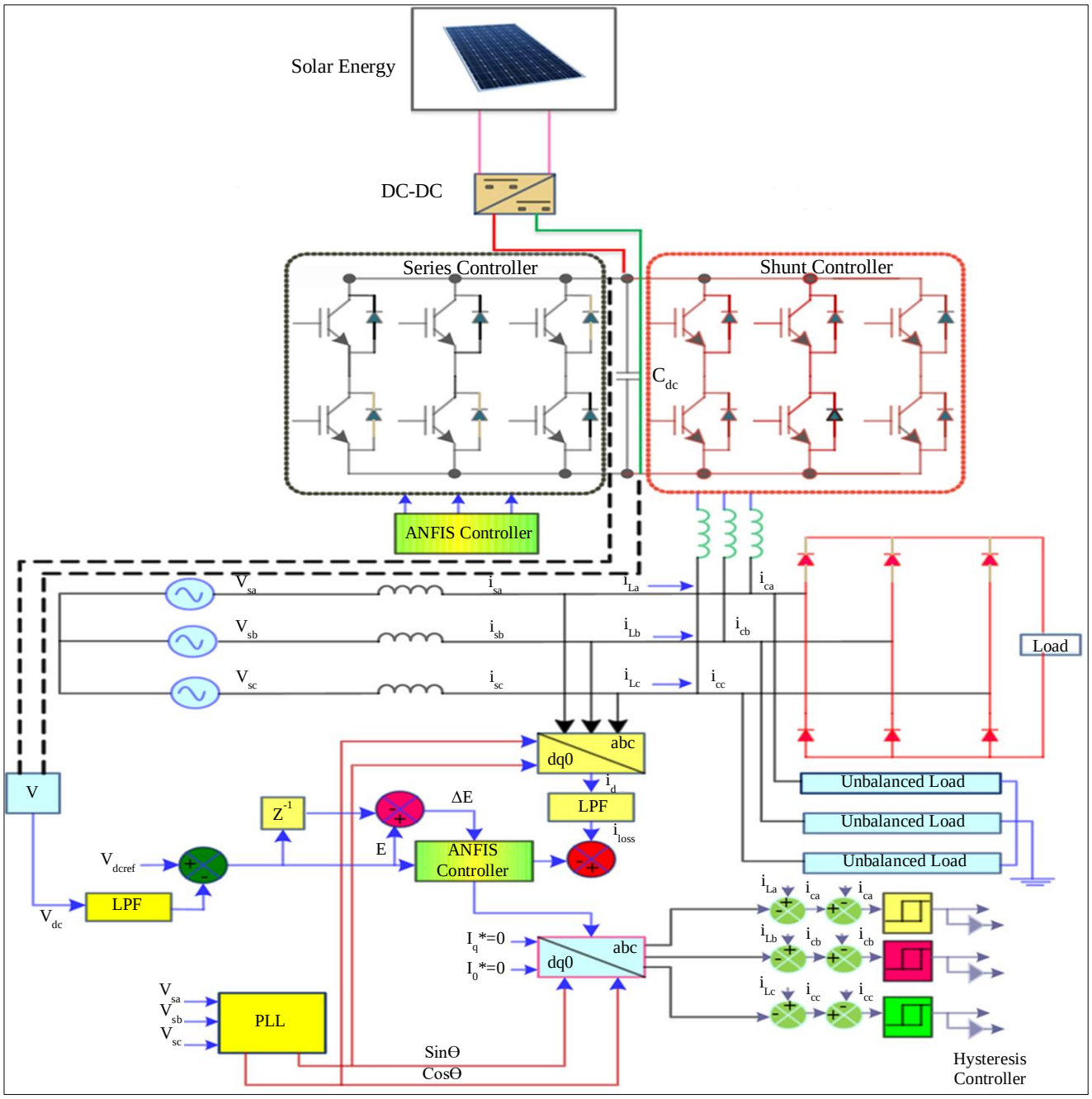

Fig. 1 The block diagram of UPQC with ANN and ANFIS

Figure 1 illustrates that Shunt APFs come in a variety of designs and categories according to their operating principle, supply, and connections (left, right, and shunt). The shunt APF adjusts for power factor, PQ problems, and current harmonics. The work examines the right shunt and applies it to the development of a unique control algorithm. Two voltage-sourced pulse width modulated inverters coupled by a DC connection comprise the PV-Shunt APF and Series APF. The photovoltaic array provides power for this DC connector. Shunt connections are made between the PWM inverter and the appropriate system device [13].

All three phases and all three wires are used to wire a nonlinear load into the system. The high switching frequency operation is what causes the ripples, and the RC filter is added to the circuit to bring the ripples down to a reasonable level. Figure 2 shows the PV Shunt APF and Series APF System [14].

2. Solar PV System

Figure 2 depicts the equivalent circuit architecture of a photovoltaic array constructed from parallel series links of PV cells. The voltage produced by a photovoltaic cell corresponding to photocurrent is primarily influenced by the charge current strength of solar radiation. A PV cell circuit comprises of diode, resistor network, and I_{LGC}.

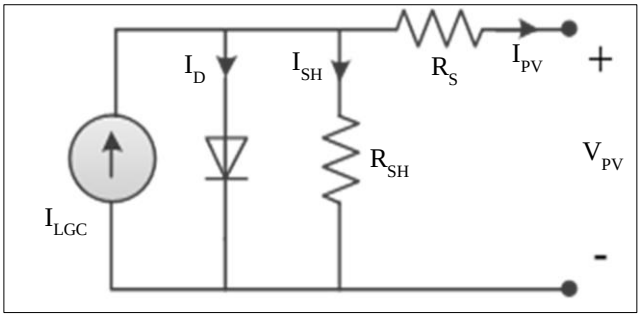

Fig. 2 Basic equivalent circuit of PV cell

The analysis technique was used to ascertain the tension and voltage produced by the group of illustrated photovoltaic cells.:

$$\text{Vseries} = \sum_{j=1}^{n} V_j = \text{V1} + \text{V2} + \cdots \ldots \ldots \ldots + \text{Vn} \quad (1)$$

$$V_{seriesoc} = \sum_{j=1}^{n} V_j = V_{oc1} + V_{oc2} + \cdots + V_{ocn} \text{ for I} = 0 \quad (2)$$

$$I_{parallel} = \sum_{j=1}^{n} I_j = I_1 + I_2 + \ldots\ldots\ldots + I_n \quad (3)$$

$$V_{parallel} = V_1 = V_2 = \ldots\ldots = V_n \quad (4)$$

Solar panels typically incorporate bypass diodes in order to reduce the quantity of surplus voltage. However, this does increase the cost of the system.

3. Mathematical Modeling

3.1. Shunt APF

The d-q approach is used to create the control strategy indicated below. Shunt-APF aids in

a) Lowering the I_L reactive component, and
b) To regulate the voltage of the capacitor in the common DC-link, hence improving the dynamic performance and lower THD.

The load current (i_{l_abc}) was translated into a d-q reference frame by using.

$$i_{l_{dq0}} = \mathrm{T}_{ryb}^{dq0} * i_{l_{ryb}} \quad (5)$$

In Equation (5), the transformation values are given.

$$\mathrm{T}_{ryb}^{dq0} = 2/3 \begin{bmatrix} coswt & \cos(wt - 120^{\circ}) & \cos(wt + 120°) \\ sinwt & \sin(wt - 120°) & \sin(wt + 120°) \\ 1/2 & 1/2 & 1/2 \end{bmatrix} \quad (6)$$

LPFs can be obtained by transforming the +ve sequence component into dc values in the d-q axis.

$$i_{l\_d} = \bar{\imath}_{l\_d} + \hat{\imath}_{l\_d} \quad (7)$$

$$i_{l\_q} = \bar{\imath}_{l\_q} + \hat{\imath}_{l\_q} \quad (8)$$

Where i_{l_d} and i_{l_q} are currents at the load's d-q element, the ac dc quantities of the d-q elements are expressed as values.

The feeder current can be computed using the values of i_l and i_{pf}, i.e. $=i_l . i_{pf}$.

The shunt VSC's d-q elements are then obtained as follows:

$$i_{pf\_d}^{ref} = \hat{\imath}_{l\_d} \quad (9)$$

$$i_{pf\_q}^{ref} = \hat{\imath}_{l\_q} \quad (10)$$

As a result, the d-q component of the feeder current is,

$$i_{s\_d} = \hat{\imath}_{l\_d} \quad (11)$$

$$i_{p\_d}^{ref} = \hat{\imath}_{l\_d} + \Delta i_{dc} \quad (12)$$

PWM is then used to turn I_{ref} in (12) back into the ABC reference frame. The three-phase compensatory output current is,

$$i_{p\_q}^{ref} = \hat{\imath}_{l\_q} \quad (13)$$

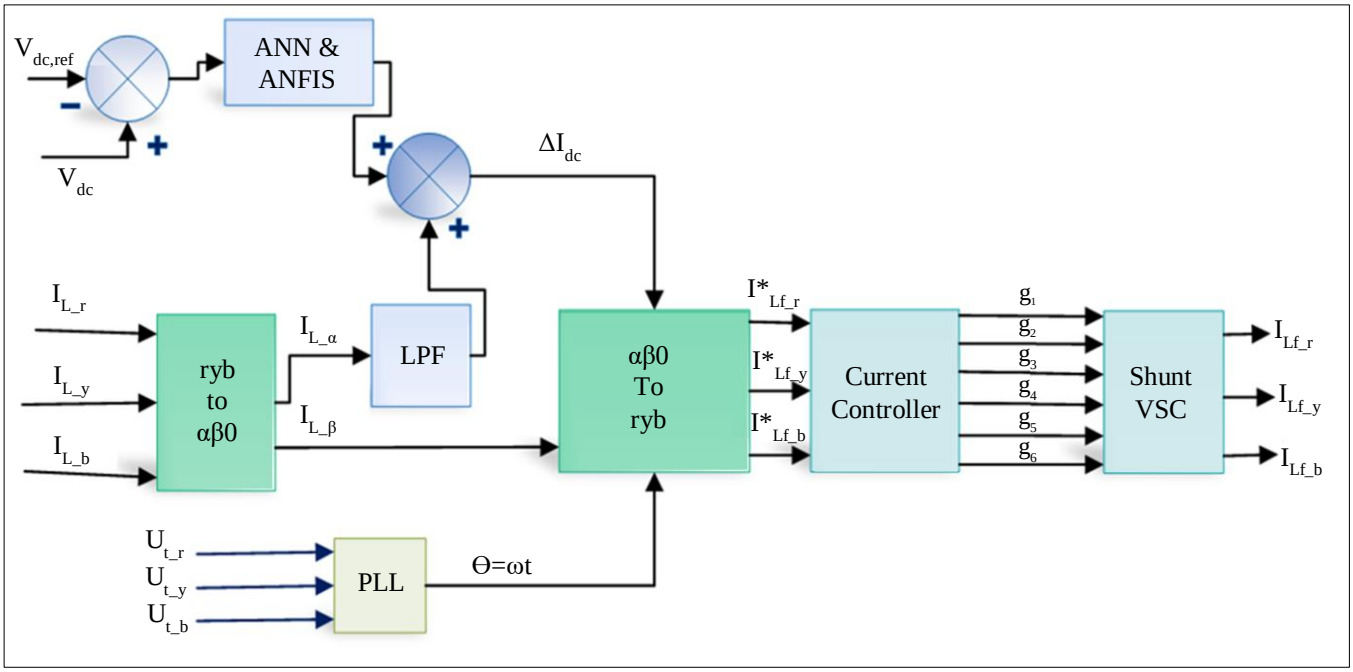

Fig. 3 Control diagram of shunt-APF

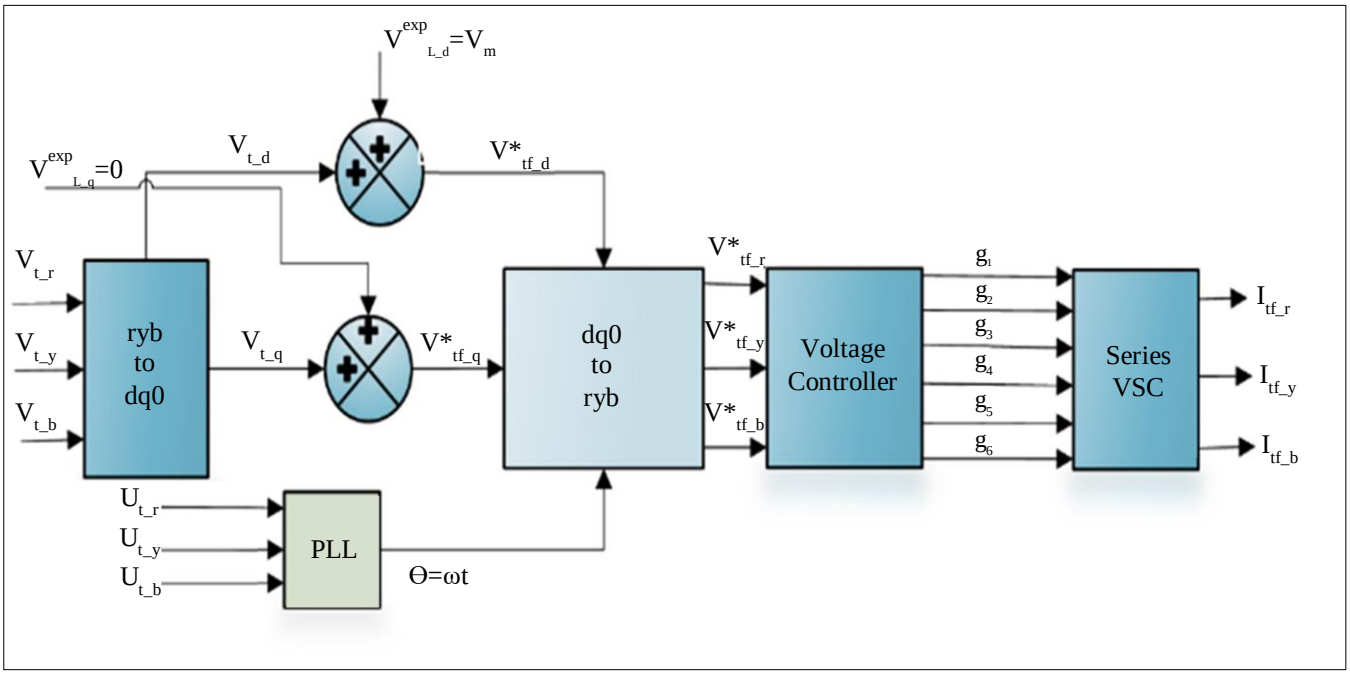

Fig. 4 Control diagram of series-APF

3.2. Series-APF

In order to lessen voltage dips and surges at the load end, series APF adds voltage in line with supply. Control activity is approximately 2 msec under oscillation conditions, ensuring a steady voltage. The feature of a series-APF is to protect sensitive loads from voltage sags or surges originating from the system-the Series-APF manages delicate loads. Series voltage is inserted to restore the load to its pre-fault value in the event that a fault arises on another line. The three inserted phases' brief magnitudes The manner in which voltages are limited reduces the negative impact of bus failure on load voltage. The Single Vector Model (SVM) serves foundation for the creation of the APF series. The warped supply is used to develop the SVM further. The series APF is depicted in Figure 4. The following parameters are controlled in each feeder using series VSC.

- Eliminate voltage quality issues like Sag and swells.
- Decrease voltage distortion and harmonics.

Figure 3 depicts the Series-APF block diagram. The bus voltage (v_{t_ryb}) is sensed and converted to the synchronous d-q reference frame.

$$i_{pf\_ryb}^{ref} = T_{dq0}^{ref} * i_{pf_{dq0}}^{ref} \;\because\; \left(T_{dq0}^{ref} = T_{ryb}^{dq0-1}\right) \quad (14)$$

$$V_{t_{dq0}} = T_{ryb}^{ref} * V_{t_{ryb}} = V_{t1p} + V_{t1n} + V_{t10} + V_{thd} \quad (15)$$

V_{t1p}, V_{t1n} and V_{t1o} are elemental frequency +ve, -ve, zero-sequence elements, V_{thd} is a harmonic element of bus voltage.

$$\begin{cases} V_{t1p} = [V_{t1p\_d} \;\; V_{t1p\_q} \;\; 0]^T \\ V_{t1n} = [V_{t1n\_d} \;\; V_{t1n\_q} \;\; 0]^T \\ V_{t10} = [0 \;\; 0 \;\; V_{t10_o}]^T \\ V_{th} = [V_{th\_d} \;\; V_{th\_q} \;\; V_{th\_0}]^T \end{cases} \quad (16)$$

$$V_{l_{dqo}}^{exp} = T_{ryb}^{ref} = T_{ryb}^{ref} * V_{l_{ryb}}^{exp} = \begin{bmatrix} V_m \\ 0 \\ 0 \end{bmatrix} \quad (17)$$

Where load voltage in the ryb reference frame($V_{l\_ryb}^{exp}$) is,

$$V_{l\_ryb}^{exp} = \begin{cases} V_m \cos(\omega t) \\ V_m \cos(\omega t - 120°) \\ V_m \cos(\omega t + 120°) \end{cases} \quad (18)$$

In a synchronous d-q reference frame ($V_{sf\_dq0}^{ref}$), compensating reference voltage is calculated as

$$V_{sf\_dq0}^{ref} = V_{t\_dq0} - V_{l_{dq0}}^{exp} \quad (19)$$

The V_{t1p_d} should be substituted in (16), kept at V_m and unneeded components are removed before being converted back to the ryb frame in (18).

4. Control Strategy

4.1. Artificial Neural Network Controller

Any system that intends to operate steadily and well must identify the disruptive forces that are creating unstable or unsettling conditions as soon as possible and make up for them. As the saying goes, "Practice makes perfect." The more a system has been used in a variety of settings, the better it will be able to identify, handle, and protect against disruptions, increasing the system's stability and performance. Regretfully, machines and gadgets lack intelligence and do not acquire knowledge; instead, they execute tasks swiftly and according to a preprogrammed sequence [15]. When the system is able to learn from its working experience in addition to its rapid consecutive functioning, it can significantly boost both performance quality and operation speed. Giving the machine this ability is the Artificial Intelligence (AI) primary objective. One AI technology that finds great use in powering electronic system control is Artificial Neural Networks (ANNs).

According to a recent study, controllers built using Artificial Neural Networks (ANNs) offer converter systems enhanced stability and faster dynamic response over a broad variety of operating situations. The benefits of ANNs include huge parallelism, resilience, fast convergence, fault tolerance, contextual information processing, learning, generalization, adaptivity, and low energy consumption [16]. Figure 5 depicts the three-layer basic ANN design

1. Input layer: this layer receives and stores input data as well as inputs to be sent to the system
2. Hidden layer: this layer processes the inputs from the input layer based on the activation function, bias, and weights of the connections between the layers.
3. Output layer: this is where the computed results are kept [17].

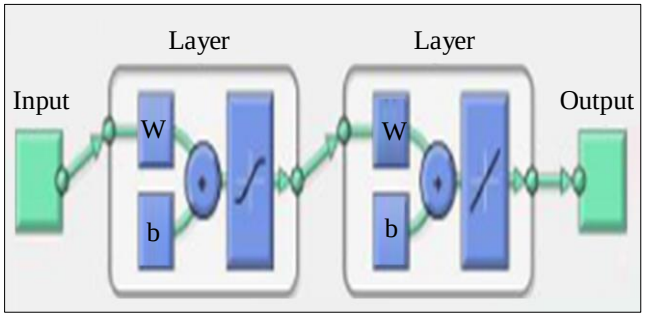

Fig. 5 Basic ANN structure

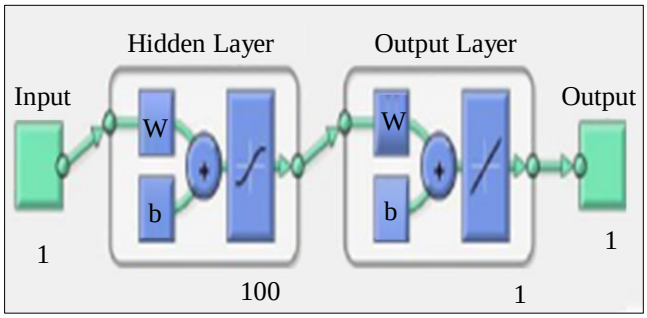

Fig. 6 ANN architecture for voltage balancing of capacitors

When mean square error is the efficiency function, Levenberg-Marquardt Back Propagation (LMBP) is one ANN training technique that offers faster convergence [18-20]. It is a feedback multidimensional network that changes weights using its produced derivatives, which sets it apart from the well-known error propagation method. The input layer input to hidden layers is provided by weights that are allocated to individual links. According to the activation function's confirmation that a node has received the full strength of

input, nodes in the concealed layer fire the inputs they provide to the output layers. When there is an error, the link weights are modified backwards so that the correct outputs are acquired for the next input iteration. The outcome verifies the result with the targets. It continues in this manner until completion.

1. In the MATLAB workspace, use the command "tool" to launch the Neural Network training tool.
2. To build the NN to control the APFs, i/p and desired data must be supplied to the ANN. The desired data and planned input have been imported and stored in the network's construction environment.
3. Of the data supplied for the targets and inputs, 70%, 15%, and 15% are used for the network's testing, validation, and training, respectively.
4. An ANN network with a given number of hidden layers will be developed using the ANN tool.
5. Using Levenberg-Marquardt backpropagation, the network will now be trained for the supplied input and target data by the training command (trainlm). Using the provided data, it verifies and tests the network.
6. Upon training completion, the tool generates the Simulink network upon command.

5. ANN-Based Shunt Controller

A similar process to that covered in Section 3.1 is used in the shunt controller to train the network to generate reference signals and maintain a constant voltage in the DC link capacitor. To keep capacitor voltage balancing, the Artificial Neural Network (ANN) predicts the output or loss component of current (I∗dc) and feeds this information to the network as the desired data.

The actual voltage Vdc is compared to the reference voltage (700 V), and the error that results from this comparison is used as the input information. As shown in Figure 6, the network that was trained employs the Levenberg-Marquardt backpropagation technique to fine-tune its size with 100 enclosed layers.

The projected reference currents provide the system with goal information even if the load currents (I_{La}, I_{Lb}, and I_{Lc}) and the current loss module (I∗dc) are considered input data for the purpose of creating the reference currents. The network that was trained to employ the Levenberg-Mar backpropagation method is displayed in Figure 7; a network with 200 hidden layers can have its size changed. The balancing DC link voltage and generating I_{ref} using ANN is displayed in Figure 8.

To produce precise switch pulses for a 3-level shunt converter, as revealed in Figure 9, the actual shunt incorporating currents is compared with the corresponding reference shunt introducing currents within limits.

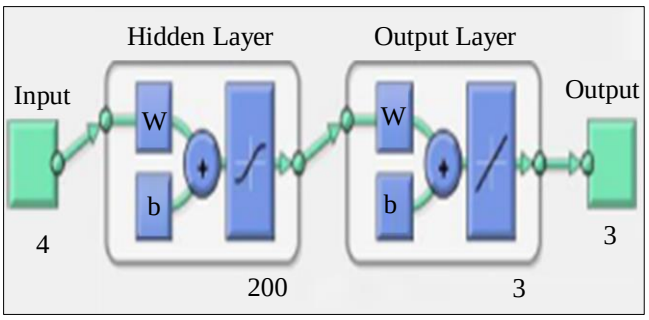

Fig. 7 ANN structure

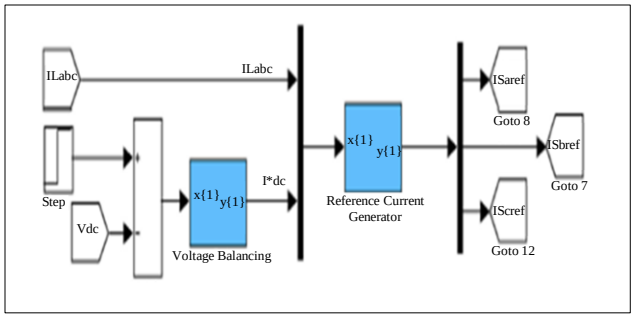

Fig. 8 Voltage stabilization of capacitors and production of a reference current

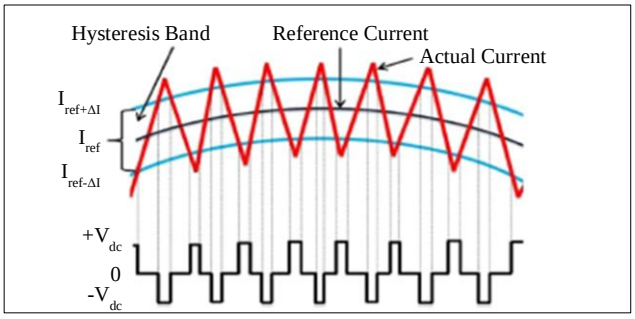

Fig. 9 Controller for hysteresis current

5.1. ANN-Based Series Controller

The projected current references serve as goal data by the network, while the voltages supplied (V_{Sa}, V_{Sband}, and V_{Sc}) are used as input information to construct the reference voltages. The system's size can be changed thanks to its 200 hidden layers.

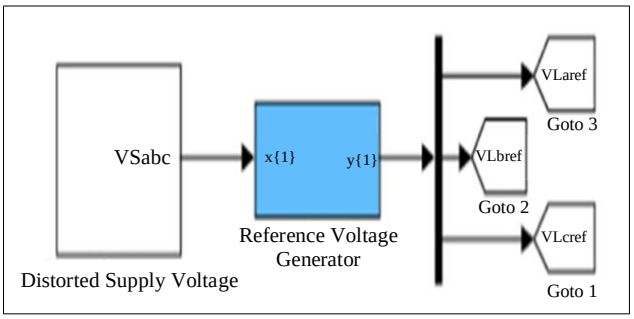

Fig. 10 Methodology for the creation of reference voltage

The model for the Artificial Neural Network (ANN) that produces a reference voltage is displayed in Figures 10 and 11 shows the Levenberg-Marquardt back propagation algorithm-trained network. There is a comparison between the reference voltages produced by the ANN supervisor and the concrete supply voltages. Using SPWM, gating pulses for the converter's series input will be produced in response to the relevant error signal.

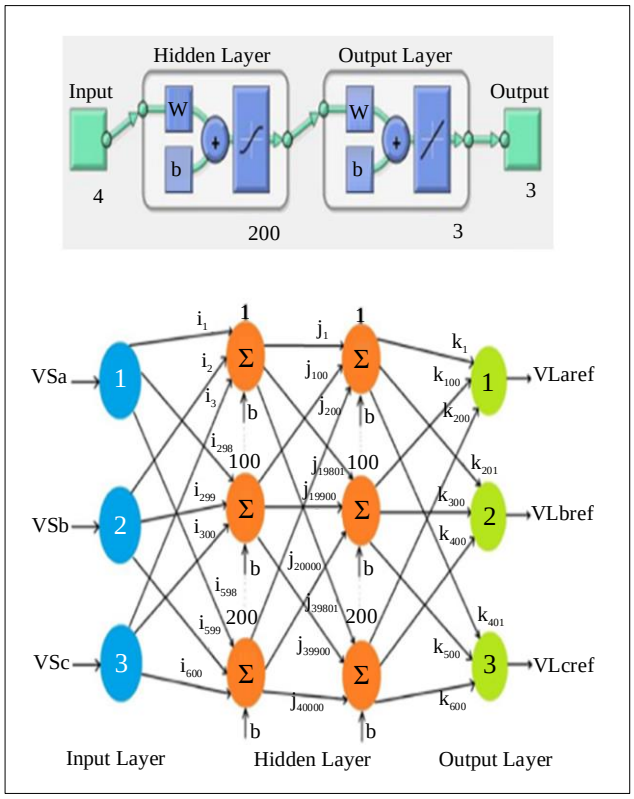

Fig. 11 A backpropagation network's design

6. Simulation Results

6.1. Current Compensation with PI Controller

As seen in Figure 12, the input current becomes sinusoidal when PI-based UPQC is used. Harmonics are currently taken good care of. Figure 13 displays the results of the simulation for the source, load, and filter currents with FLC.

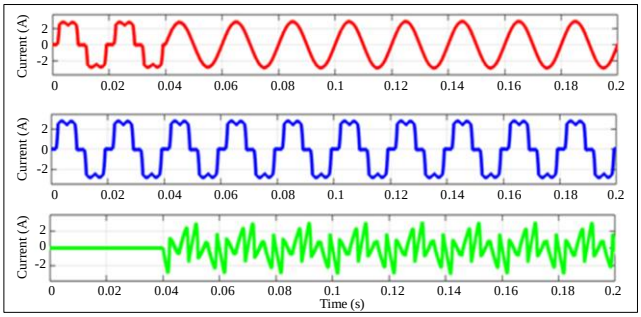

Fig. 12 I_s, I_L and I_f with PI

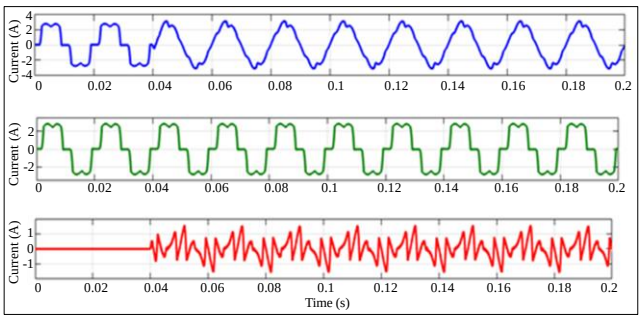

Fig. 13 Is, I_L and I_f with FLC method

6.2. Voltage and Current of Source after Compensation

The simulation for source voltage, source current, load voltage, and load current with ANN is displayed in Figure 14. It was found that the source and load sides' voltages and currents were properly balanced following the implementation of ANN.

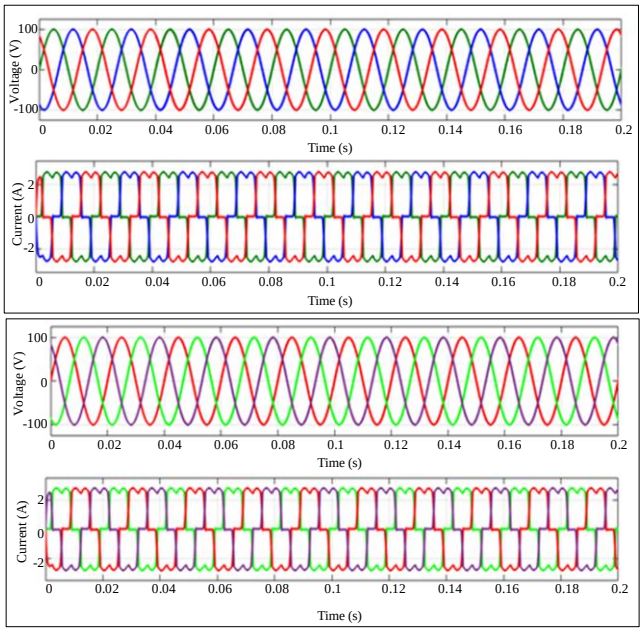

Fig. 14 V_s, Is V_L and I_L with the proposed method

6.3. Current Harmonics Compensation with ANN & ANFIS

The result of Current harmonics Compensation with ANN and ANFIS Controller after filtering current is shown in Figures 15 and 16, respectively. The input current becomes sinusoidal after implementation of ANFIS controller-based Shunt APF, as shown in Figure 16. The current harmonics are well compensated. In this System, IS, IL are balanced, and distortion reduction is better compared to the ANN controller.

6.4. Voltage Swell and Sag Compensation with ANFIS

The model is run for a duration of 0.2 to 0.4 seconds, as shown in Figure 17. Voltage swells are effectively compensated for by ANFIS-based series APF.

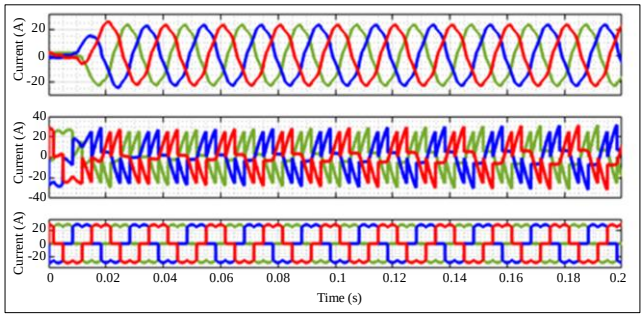

Fig. 15 Simulation result of I_S, I_f, I_L with ANN

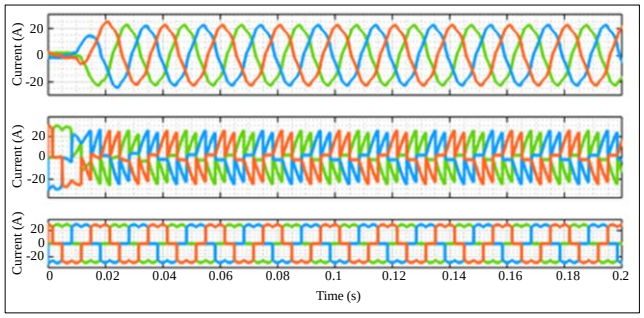

Fig. 16 Simulation result of I_S, I_f and I_L with ANFIS

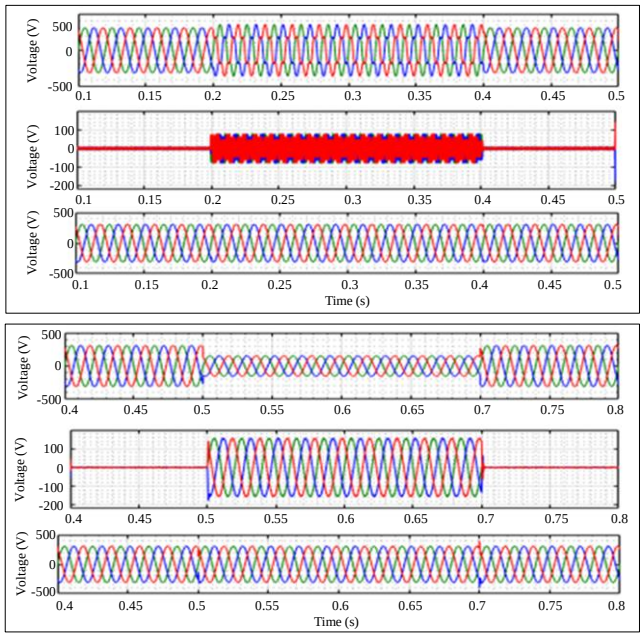

Fig. 17 Voltage swell during 0.2 to 0.4 sec, sag during 0.5 to 0.7 sec with ANFIS

Figure 17 illustrates how the swell scenario affects power generation. After employing ANFIS based series APF, Swell remains unaffected. The first waveform of the graph shows a source voltage with a swell, and the third waveform shows the voltage injection; the waveforms are together, subsequent graph shows rectified V_L. As seen in Figure 17, A Sag develops throughout 0.5 to 0.7 seconds. Adaptive ANFIS-based series APF reduces the loss of return, as seen in Figure 17. The APF series based on Adaptive ANFIS does not affect Sag. The first shows the tension in the network with Sag, the third shows the added tension, and the second shows the modified tension of the load.

6.5. Voltage Swell and Sag Compensation with ANN

The model is run for a duration of 0.2 to 0.4 seconds, as shown in Figure 18. Voltage swells are effectively compensated for by ANN-based series APF. Figure 18 illustrates how the swell scenario affects power generation. After employing ANN based series APF, Swell remains unaffected. The first waveform of the graph shows a grid voltage with the swell, the third waveform appears as the injected voltage, and when both waveforms are combined, the subsequent waveform shows the rectified V_L. As seen in Figure 18, A Sag develops throughout 0.5 to 0.7 seconds. Adaptive ANN-based series APF reduces the loss of return, as seen in Figure 18. The APF series based on Adaptive ANN does not affect Sag. The first shows the tension in the network with Sag, the third shows the added tension, and the second shows the modified tension of the load.

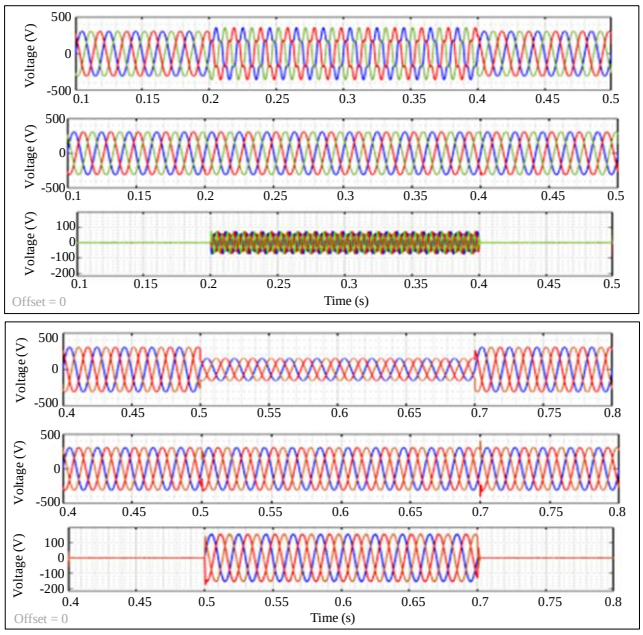

Fig. 18 Voltage swell during 0.2 to 0.4 sec, Sag during 0.5 to 0.7 sec with ANN

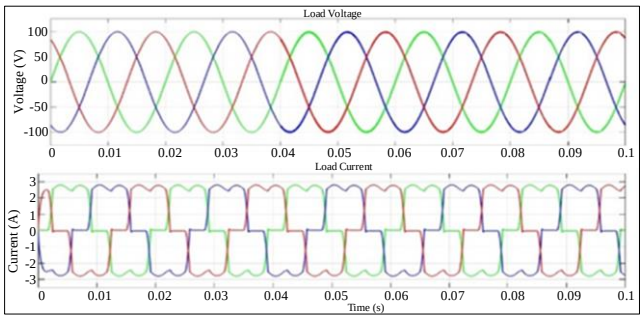

Fig. 19 Simulation result of compensated V_L, I_L with ANFIS

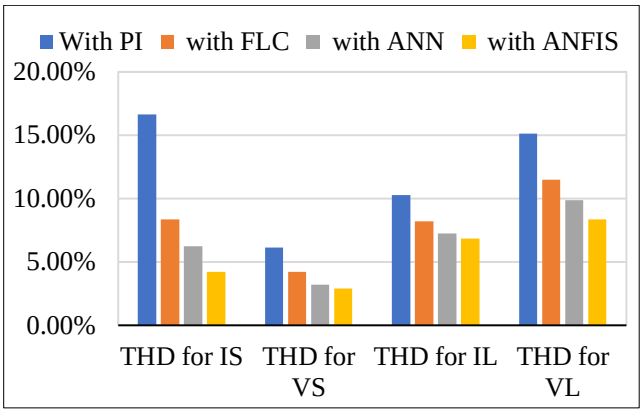

Fig. 20 Comparison result of THD with different controllers

Figure 19 shows the simulation results of load voltage and load current with the ANFIS controller. Table 1 shows the comparative analysis of source current, source voltage, load current and load voltage with various controllers, which indicates that the total harmonic distortion for all the above parameters is the least with the ANFIS controller. In the result analysis after examining the system with different controllers. The ANFIS controller has given good dynamic performance and improved the power quality in terms of THD so that the system can achieve the desired output without any disturbances.

Table 1. THD results for IS, Vs, IL and VL

Controllers	Parameters			
	THD for I_S	THD for V_S	THD for I_L	THD for V_L
With PI	16.63%	6.14%	10.30%	15.14%
With FLC	8.35%	4.21%	8.21%	11.5%
With ANN	6.24%	3.21%	7.23%	9.86%
With ANFIS	4.24%	2.91%	6.85%	8.38%

7. Conclusion

In this chapter, ANN and ANFIS-based UPQC integrated with solar DC link voltage is suggested to address PQ issues such as the regulation of VDC-Link (performance parameters), as well as harmonic compensation, Voltage fluctuations and THD for Vs, V_L, Is, and I_L with ANN and ANFIS, as well as the learning part and flowchart of the proposed Controller. On a power distribution network with nonlinear loads, the performance of Shunt, Series APF is demonstrated. In comparison to solar fed UPQC with ANN controller, UPQC with ANFIS controller is much better in improving dynamic performance and power quality.

References

[1] Srinivas Nakka, R. Brinda, and T. Sairama, "Design and Simulation of Six-Phase UPFC Power Quality Enhancement with Improved GWO-Based Decoupled Power Control Strategy," *International Journal of System Assurance Engineering and Management*, vol. 14, pp. 2605-2625, 2023. [CrossRef] [Google Scholar] [Publisher Link]

[2] Dipak R. Swain et al., "Optimal Fractional Sliding Mode Control for the Frequency Stability of a Hybrid Industrial Microgrid," *AIMS Electronics & Electrical Engineering*, vol. 7, no. 1, pp. 14-37, 2023. [CrossRef] [Google Scholar] [Publisher Link]

[3] D. Krishna, M. Sasikala, and R. Kiranmayi, "FOPI and FOFL Controller Based UPQC for Mitigation of Power Quality Problems in Distribution Power System," *Journal of Electrical Engineering and Technology*, vol. 17, pp. 1543-1554, 2022. [CrossRef] [Google Scholar] [Publisher Link]

[4] Shawon Das et al., "Empirical Analysis of Power Quality Using UPQC with Hybrid Control Techniques," *Results in Engineering*, vol. 20, 2023. [CrossRef] [Google Scholar] [Publisher Link]

[5] D. Krishna, M. Sasikala, and V. Ganesh, "Fractional Order Fuzzy Logic Based upon for Improvement of Power Quality in Distribution Power System," *International Journal of Recent Technology and Engineering*, vol. 7, no. 6, pp. 1405-1410, 2019. [Publisher Link]

[6] Jyothi Nemmadi, and M. Manjula, "Shunt Active Power Filter for Power Quality Enhancement of Distribution Power System Using Fuzzy Logic Controller," *Proceedings of the Second International Conference on Emerging Trends in Engineering*, pp. 548-556, 2023. [CrossRef] [Google Scholar] [Publisher Link]

[7] Hossein Toopchizadeh et al., "An Effective Shunt Active Power Filter Based on Novel Binary Multi-Level Inverter and Optimal Type-2 Fuzzy System to Accurately Mitigate Harmonic Currents," *Evolving Systems*, vol. 14, pp. 783-800, 2023. [CrossRef] [Google Scholar] [Publisher Link]

[8] D. Krishna, M. Sasikala, and V. Ganesh, "Adaptive FLC-Based UPQC in Distribution Power Systems for Power Quality Problems," *International Journal of Ambient Energy*, vol. 43, no. 1, pp. 1719-1729, 2022. [CrossRef] [Google Scholar] [Publisher Link]

[9] S. Narthana, and J. Gnanavadivel, "Power Quality Analysis of Interleaved Cuk Configuration-Based Interval Type-2 Fuzzy Logic Controller for Battery Charging in Electric Vehicles," *Arabian Journal for Science and Engineering*, vol. 49, pp. 6259-6273, 2024. [CrossRef] [Google Scholar] [Publisher Link]

[10] Surendra Kumar Sharma, Ashish Raj, and Sunil Kumar Gupta, "Investigations on Power Quality Improvement Using Soft Computing Based Unified Power Quality Conditioner," *AIP Conference Proceedings*, vol. 2782, 2023. [CrossRef] [Google Scholar] [Publisher Link]

[11] E. Parimalasundar et al., "Artificial Neural Network-Based Experimental Investigations for Sliding Mode Control of an Induction Motor in Power Steering Applications," *International Journal of Intelligent Systems*, vol. 2023, pp. 1-14, 2023. [CrossRef] [Google Scholar] [Publisher Link]

[12] Vikas Khare, and Pradyumn Chaturvedi, "Design, Control, Reliability, Economic and Energy Management of Microgrid: A Review," *e-Prime-Advances in Electrical Engineering, Electronics and Energy*, vol. 5, 2023. [CrossRef] [Google Scholar] [Publisher Link]

[13] Ch Srivardhan Kumar, and Z. Mary Livinsa, "Development of a Novel Harris Hawks-Based Optimization Algorithm for Power Quality Enhancement in Distribution Systems Using a Dynamic Voltage Restorer," *Electrical Engineering*, vol. 150, pp. 3105-3119, 2023. [CrossRef] [Google Scholar] [Publisher Link]

[14] M. Thenmozhi et al., "Design and Implementation of Photovoltaic-Assisted Dynamic Voltage Restorer Using Fuzzy Logic Controller-Based Improved SOGI for Power Quality Improvement," *Electrical Engineering*, 2023. [CrossRef] [Google Scholar] [Publisher Link]

[15] S.T. Siddharthan, and A. Shunmugalatha, "A Robust Approach for Mitigating Load Voltage Imbalances Using Glowworm Swarm Optimizer for Power Quality Enrichment," *Electric Power Systems Research*, vol. 229, 2024. [CrossRef] [Google Scholar] [Publisher Link]

[16] Chandrakala Devi Sanjenbam, Bhim Singh, and Priyank Shah, "Reduced Voltage Sensors Based UPQC Tied Solar PV System Enabling Power Quality Improvement," *IEEE Transactions on Energy Conversion*, vol. 38, no. 1, pp. 392-403, 2023. [CrossRef] [Google Scholar] [Publisher Link]

[17] K. Thanigaivel, S. Ramesh, and K. Karunanithi, "A Hybrid DMO-RERNN Based UPFC Controller for Transient Stability Analysis in a Grid-Connected Wind-Diesel-PV Hybrid System," *International Review of Applied Sciences and Engineering*, vol. 14, no. 3, pp. 325-341, 2023. [CrossRef] [Google Scholar] [Publisher Link]

[18] P. Vivek, and N.B. Muthu Selvan, "Experimental Investigation on a Solar Photovoltaic System Using Reduced Multi-Level Connections for Power Quality Improvement," *Electrical Engineering*, vol. 105, pp. 2889-2908, 2023. [CrossRef] [Google Scholar] [Publisher Link]

[19] Md Shafiul Alam, "Solar and Wind Energy Integrated System Frequency Control: A Critical Review on Recent Developments," *Energies*, vol. 16, no. 2, pp. 1-31, 2023. [CrossRef] [Google Scholar] [Publisher Link]

[20] Krishna Sarker, "FC-PV-Battery-Z Source-BBO Integrated Unified Power Quality Conditioner for Sensitive Load & EV Charging Station," *Journal of Energy Storage*, vol. 75, 2024. [CrossRef] [Google Scholar] [Publisher Link]

[21] Ze-Yin Zheng, Hao-Yu Qiu, and Mou-Fa Guo, "Phase-Segregated Injection Method for Arc Suppression with Cascaded H-Bridge Inverters Considering Line Voltage Drop," *SSRN*, pp. 1-11, 2023. [CrossRef] [Google Scholar] [Publisher Link]

[22] Amirullah Amirullah, and Adianand Adianand, "Single Phase UPQC Integrated with Photovoltaic System without DC-Link Capacitor Using Fuzzy Logic Controller for Power Quality Improvement," *International Journal of Intelligent Engineering and Systems*, vol. 16, no. 3, pp. 1-18, 2023. [Google Scholar] [Publisher Link]